AWARD NUMBER: W81XWH-19-1-0468

TITLE: Drug-Induced Regeneration and Re-Innervation in a Mouse Digit Amputation Model

PRINCIPAL INVESTIGATOR: Phillip Messersmith, Ph.D.

CONTRACTING ORGANIZATION: University of California, Berkeley, CA

REPORT DATE: November 2023

TYPE OF REPORT: Final

PREPARED FOR: U.S. Army Medical Research and Development Command
Fort Detrick, Maryland 21702-5012

REPORT DOCUMENTATION PAGE

Form Approved
OMB No. 0704-0188

1. REPORT DATE	2. REPORT TYPE	3. DATES COVERED
November 2023	Final	01Aug2019-31Jul2023

4. TITLE AND SUBTITLE

Drug-Induced Regeneration and Re-Innervation in a Mouse Digit Amputation Model

5a. CONTRACT NUMBER
W81XWH-19-1-0468

5b. GRANT NUMBER
PR180789P1

5c. PROGRAM ELEMENT NUMBER

6. AUTHOR(S)

Phillip B. Messersmith

E-Mail: philm@berkeley.edu

5d. PROJECT NUMBER

5e. TASK NUMBER

5f. WORK UNIT NUMBER

7. PERFORMING ORGANIZATION NAME(S) AND ADDRESS(ES)

The Regents of the University of California
c/o Sponsored Projects Office
1608 Fourth Street, Suite 220
Mail Code 5940
University of California, Berkeley, CA 94710-1749

8. PERFORMING ORGANIZATION REPORT NUMBER

9. SPONSORING / MONITORING AGENCY NAME(S) AND ADDRESS(ES)

U.S. Army Medical Research and Development Command
Fort Detrick, Maryland 21702-5012

10. SPONSOR/MONITOR'S ACRONYM(S)

11. SPONSOR/MONITOR'S REPORT NUMBER(S)

12. DISTRIBUTION / AVAILABILITY STATEMENT

Approved for Public Release; Distribution Unlimited

13. SUPPLEMENTARY NOTES

In the proposed studies, we have used our experience in soft and hard tissue regeneration induced by the HIF1α-stabilizing drug, 1,4-DPCA, in a drug delivery system (PEG-DPCA nanogel) towards therapies for hand, nerve, and digit regeneration. In the current studies, we are exploring the effect of this drug on 1) digit regrowth post-amputation and nerve regeneration, 2) drug effects on peripheral re-innervation in rat forelimbs after injury and 3) optimization of drug potency and delivery in these systems. Our progress during this third year includes studies on surgically-amputated digits in mice using Micro-CT analysis showing changes with 1,4-DPCA drug therapy with and without BMP2. Significant changes at 3 months showed changes in bone density and volume. In the Tuffaha/Brandacher model of rat forelimb nerve resection, using larger rat cohorts than previously reported, we again showed drug-enhanced grip strength, reduced muscle atrophy, and nerve fiber regeneration.
During this no-cost extension year, we will explore multiple drug injections for longer periods of time, new dosing, effects of BMP2 addition post-digit amputation, continue studies in forelimb nerve regrowth, effects on digit function, further development of the 1,4-DPCA drug delivery system and modification of 1,4-DPCA compounds.

15. SUBJECT TERMS
BMP2; Bone Mineral Density; Bone Volume; 1,4-DPCA; Digit Amputation: Flexor digitorum profundus (FDP), Grip Strength Analysis; Micro-CT Analysis; Muscle Atrophy; Nerve Co-aptation; Nerve Regeneration

16. SECURITY CLASSIFICATION OF:			17. LIMITATION OF ABSTRACT	18. NUMBER OF PAGES	19a. NAME OF RESPONSIBLE PERSON
a. REPORT	b. ABSTRACT	c. THIS PAGE			USAMRDC
Unclassified	Unclassified	Unclassified	Unclassified	19	19b. TELEPHONE NUMBER *(include area code)*

TABLE OF CONTENTS

INTRODUCTION

The ability to regenerate bone, nerve, and other soft tissue has been the focus of our laboratories for the past 25 years, ever since discovering the spontaneously regenerating MRL mouse. With genetic mapping studies, gene expression studies, exploring early events in the response, we (the **Heber-Katz Laboratory, LIMR**) determined the effect of the metabolic state on the formation of a regeneration blastema. Mitochondria in the MRL mouse had low membrane potentials, similar to what one sees in stem cell niches, embryonic tissue, and tumors. This causes an aerobic glycolytic (AG) state, unlike the OXPHOS seen in adult mature tissue. A major gene that regulates AG, HIF-1a, was found to be highly expressed in MRL mice after injury. We could silence this gene using siRNA which turned off MRL regenerative responses. But, could we turn on HIF-1a in a non-regenerative mouse and achieve regeneration? Together with **Phillip Messersmith** (**UC Berkeley Laboratory**), an expert in materials science and the co-PI of this grant proposal, who created a HIF-1a stabilizing small molecule with a delivery system, we could modulate HIF-1a levels and induce regeneration in non-regenerative mice. In this proposal, we explored the effect of this small molecule drug on digit growth post-amputation, as well as nerve re-growth after transection, re-establishment of digit movement and grip strength in collaboration with a hand surgeon, **Dr. Aviram Giladi, MD (the Curtis Hand Center Laboratory, Baltimore).**

KEY WORDS

1,4-DPCA-PEG, C57BL/6 x129 Mice, Digit Amputation, Sprague Dawley Rats, Motor Sensory Nerve Regeneration, Muscle Atrophy, Scar Formation, Grip Strength

ACCOMPLISHMENTS

What were the major goals of the project?

There are 4 major goals of this project as stated in the SOW:

1. We will determine the effect of drug/gel using different doses and added drug injections over time or any new drug formulations on nerve regeneration at terminal sites in the mouse digit after amputation.
2.We will examine healing across nerves ends after transection in the forelimb, and track nerve recovery in the rat using different injury models and drug dosages.
3. We will synthesize and characterize 1,4-DPCA-PEG Conjugates in vivo and in vitro.
4.We will synthesize and characterize 1,4-DPCA-Peptoid Conjugates.

Figure 1

What was accomplished under these goals?

We carried out two types of injuries**.** The first was a mouse digit amputation to examine the effect of the DPCA-PEG drug on regrowth of bone. The second was the transection of PNS nerves in the rat forelimb to determine if the DPCA-PEG drug could accelerate nerve re-growth, digit movement, and grip strength.

I) We examined the effect of the DPCA drug on digit growth after amputation in the 2nd phalange seen in **Fig 1**. DPCA-PEG was administered systemically by injecting SQ in the mouse flank. The second phalanx of the middle digit from the hind-paw was surgically amputated midway between the proximal and distal joints under isoflurane and buprenorphine administered every 8 hours. These mice were followed for 6 months using microCT analysis after receiving one round of DPCA-PEG. At this time, we also carried out immunohistochemistry to examine nerve, tendon, and bone growth.

In the micro CT scans in **Fig 2**, one can see the formation of the radiodense region or “callus”. In this experiment, the callus is seen as early as day 14 and may have formed between days 7 and 14. This is true for both the experimentals (**A**) and controls (**D**). However, we see that the formation of the callus changes in location in drug-treated versus controls. Thus, the callus is more central to the amputated digit in the control, but is located near the cut end in the mice getting drug. This cut-end location could very well add to the length increase in the digit and be of biological importance for regeneration.

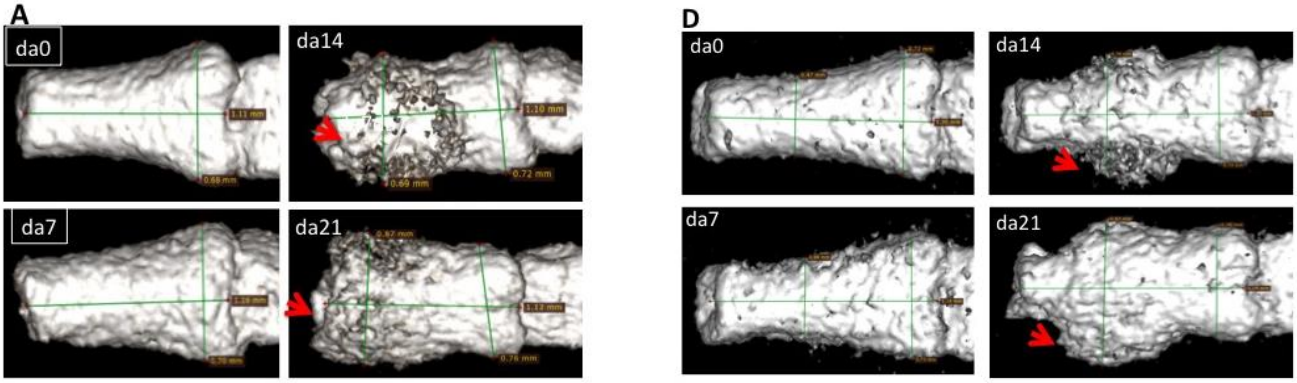

Fig 2. Analysis of the Boney Callus. In the first quartet of pictures from a mouse that received drug on days 0 and 8 (A), Micro-CT scans of da0, da7, da14, and da21 show that the bony callus forms sometime between day 7 and 14 and continues to day 21. The next panel (D) is from a control mouse receiving no drug. We did not see changes in bone length in either case. These experiments were carried out using B6/129 mice.

We did show differences in bone length after DPCA-PEG in our next experiment (**Fig 3**). In some cases, we saw an increase in bone circumference and density but little bone lengthening.

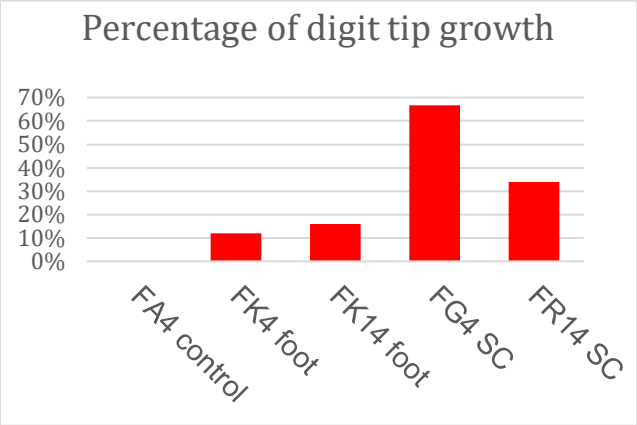

Fig 3. Changes in Bone Length. Bone length changes after amputation and 6 months after amputation comparing local vs systemic drug. Here, no change in growth was seen in the control, small differences (10-20%) were seen with local injection of drug (FK4 foot, FK14 foot), and larger effects (30-70%) were seen with distal SC (subcutaneously) drug delivery in the flank (FG4 SC, FR14 SC).

We thought that by adding BMP2, previously described to enhance bone growth (ref), we might enhance our response. We saw little difference or a negative effect.

In **Fig 4**, analysis of digit tissue post amputation showed interesting immune-staining with nerve markers. Digit sections from mice that had undergone digit amputation 6 months earlier were used. We compared H&E sections to sections stained with anti-NF (nerve fibers) and anti-Gap 43 (nerve endings) antibodies and found several striking features. In particular, only in the mice given drug SQ, was there a circular staining pattern that looked very similar to that of a joint potentially forming at the cut end (**Fig 4D,E**). A comparison to a preformed joint (**Fig 4B)** shows that the structure has a very similar shape.

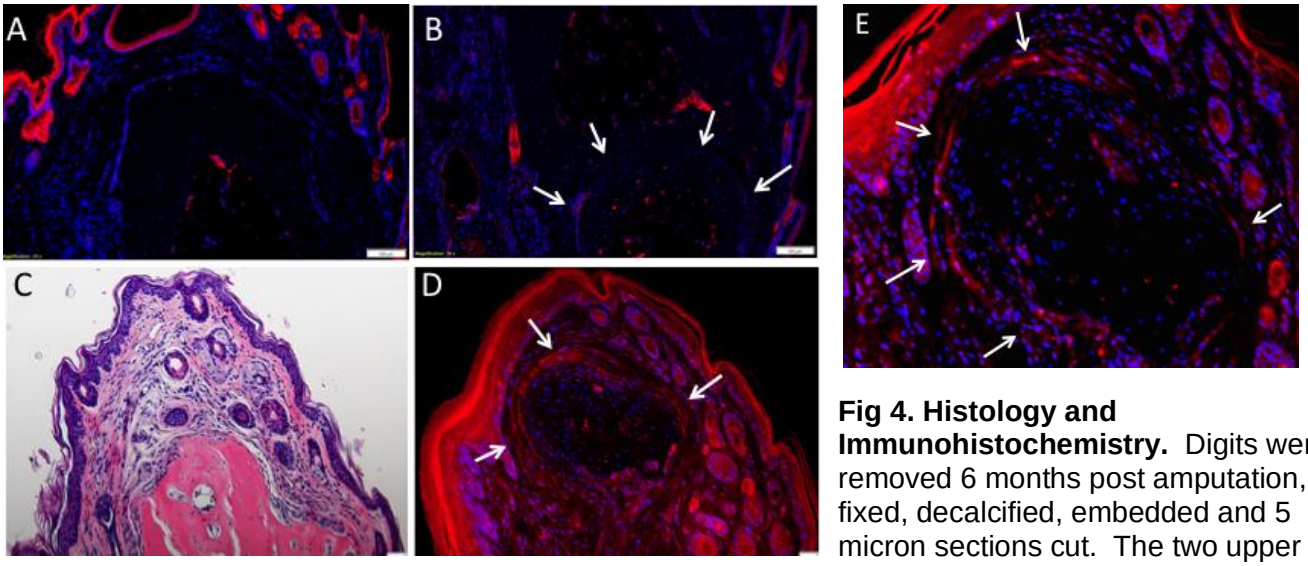

Fig 4. Histology and Immunohistochemistry. Digits were removed 6 months post amputation, fixed, decalcified, embedded and 5 micron sections cut. The two upper digit sections (A,B) were from amputated digits from mice not treated with drug (control) but stained with anti-GAP-43 antibody. In B, a pre-existing joint (white arrows point to outline) between the second and third phalanx can be seen showing no GAP-43 staining. Alternatively, an amputated digit from a mouse treated with drug subcutaneously (FR14) is shown stained with H&E (C). In D, is seen staining with anti-GAP-43. Besides high staining in hair follicles, a structure (white arrows) is stained that appears to look like a forming joint at the amputation site. This does not coincide with the existing bone seen in (C). Staining the following digit section with another antibody, anti-NF (neurofilament) antibody, shows the same structure (E).

Since data was coming in from the Giladi laboratory for Part II and regenerative response analysis was necessary, we focused our efforts to work with the Giladi group so that we could make decisions on what directions we needed to further pursue.

II) In the second study, we have analyzed the ability of DPCA-PEG to induce accelerated re-growth of damged mixed motor-sensory peripheral nerves after transection in Sprague Dawley (SD) rat forelimbs. Motor innervation of the intrinsic and extrinsic digit-activating muscles of the forelimb and paw was assessed histologically and functionally. This model is applicable to the needs of the warfighter with enhancement of digit/hand re-innervation after nerve injury.

Materials and Methods

General Methodology: Nerve transection of ulnar, median, and radial nerves in the forelimb of non-regenerating Sprague Dawley rats was carried out. Two groups included: 1) separated nerve ends were sutured to the local muscle so no nerve recovery was possible; 2) nerves were sutured together (co-aptation), permissive for nerve growth. In the first set of experiments, rats were given no drug or 2 doses of drug SQ (days 0 and 8). To assess recovery, rats were followed for up to 98 days for nerve survival and regeneration, muscle atrophy, scar formation, and recovery of lost grip strength. In a second set of experiments, we explored the effect of a second round of drug treatment.

Nerve Survival and Regeneration: Weekly samples of tissue sections from the surgical site were recovered, fixed, embedded, and sectioned 7-98 days after surgery. Microscopic analyses of tissue using histochemistry and immunohistochemistry for nerve degeneration, nerve growth, myelination, muscle degeneration, neuro-muscular junction integrity and scar formation were carried out. For example, slides from days 7, 14, 21, 41, 61, and 81 were stained with toluidine blue (a myelin stain) and then counted in a given area (4.1 mm^2) for dead and dying nerve fibers due to Wallerian degeneration (brown) and for live and newly regenerating myelinated nerve fibers (white in center).

Muscle Atrophy: Cross sections of flexor digitorum profundus (FDP) muscle/tendon were stained with anti-laminin antibody to determine fiber width and were quantified using Image J software.

Scarring Around Nerve: Proximal nerve was fixed and cross-sections cut in paraffin. Sections were stained with Picro Sirius Red (PSR). Slides were examined using polarized light and images were analyzed using ImageJ analysis.

Grip Strength: The primary measure of nerve recovery was grip strength. We used the limb stimulation approach developed by Tuffaha et al (8,9) to avoid limitations with other induced-grip techniques. Under general anesthesia, SD rats were placed in a supine position with forelimb extended. Two needle electrodes were inserted under the forelimb skin and placed on top of the nerve. A Chatillon Digital Force Gauge was attached to a trapeze-shaped grasping bar. The grasping bar was placed in the rat paw. Stimulation via electrodes prompted the rats to grip the grasping bar. Three readings were taken and expressed as Newton of Force (N) .The force gauge was then slowly pulled away. Baseline measurements were taken 1-3 days pre-operatively and every 7 days post-operatively.

Results of #II Studies in Rats

The results shown below in **Figures 1-4** all support the significant effectiveness of 1,4-DPCA/PEG as an enhancer of PNS nerve growth. We saw impressive accelerated nerve re-growth reaching higher levels than seen without drug treatment. We found that the normal state of muscle atrophy after nerve resection was reversed after the drug with larger muscle fiber area. We saw that scarring around the nerve fiber was different with and without drug and using PSR staining, it was clear that more Col I and less Col III associated with scarring was seen with drug. Finally, not just markers of healing and scarring but nerve and muscle function as seen as grip strength showed bigger differences with drug administration. In fact, the last experiment done examined the effect of injecting drug for a second round, on day 30. Most surprising was that grip strength not only returned to normal but surpassed the normal uninjured animal.

1. Nerve Survival and Regeneration (Fig 1A, below)

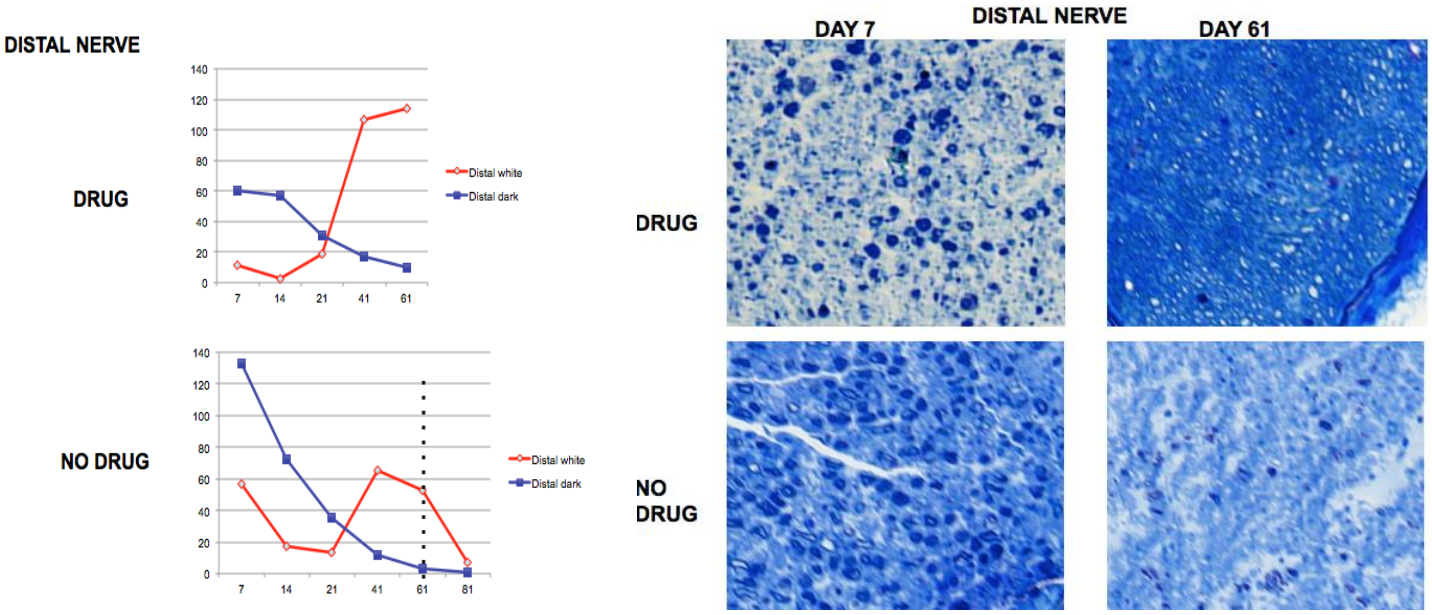

Fig 1A

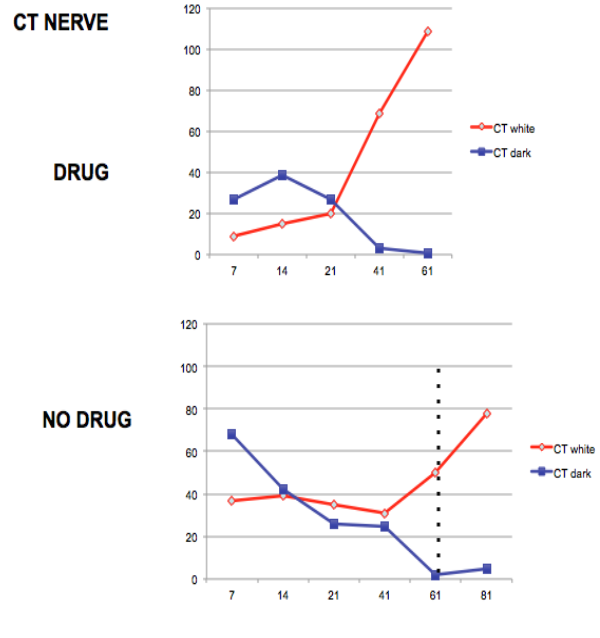

Fig 1B

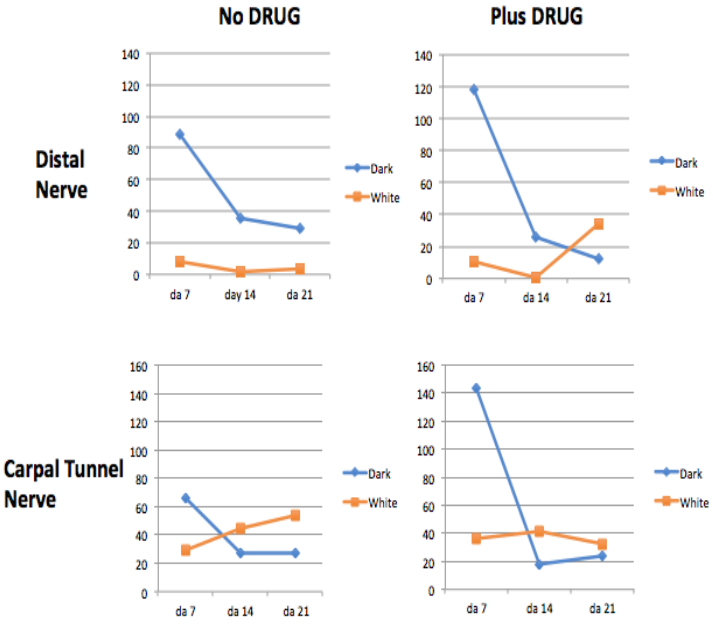

Fig1C

Figure 1: Nerve Regrowth: In **Fig 1A** In the co-apted group, dramatic regrowth of distal myelinated nerve fibers was seen in the drug-treated group increasing from 0-120 fibers/field between days 14-61. In the no drug-treated group there was an early attempt at nerve fiber regrowth between days 21-41, but the number of fibers declined after day 41 reaching 0 by day 81. Both groups showed growth of new

myelinated nerve fibers at 21 days. However, growth in the drug group was almost double at 41 days and was still increasing by 81 days whereas in the no-drug group, growth was seen at 41 days, reversed at 61 days and then new nerves disappeared by 81 days. This disappearance of nerves looks different than Wallerian degeneration with no dark neurons observed. In **Fig 1B**, the carpal tunnel (CT) nerve, near the paw, is more distal to the injury site. With drug, the appearance of new nerves began to rise at 21 days, reaching a peak at 61 days. Without drug, the number of new nerve fibers began to rise at 41 days, reaching a peak 50% of that seen with drug. Thus, at 61 days, the number of new nerve fibers with drug was 110/field whereas without drug it was 50/field. In **Fig 1C**, Wallerian degeneration occurs in the control group where the nerve is sewn to the muscle wall. This is true with or without drug in the both the distal and carpal tunnel nerves. However, in both groups, drug administration slows the rate of degeneration.

2. Muscle Atrophy

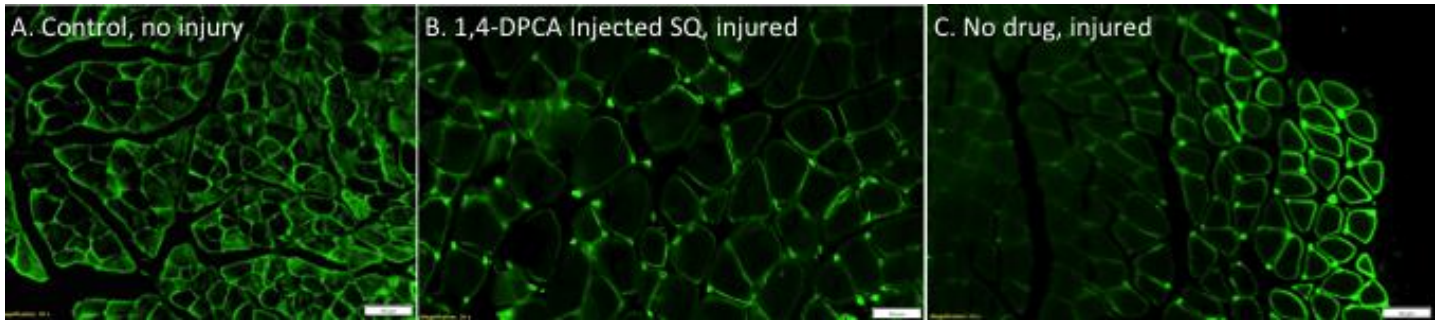

Fig 2D

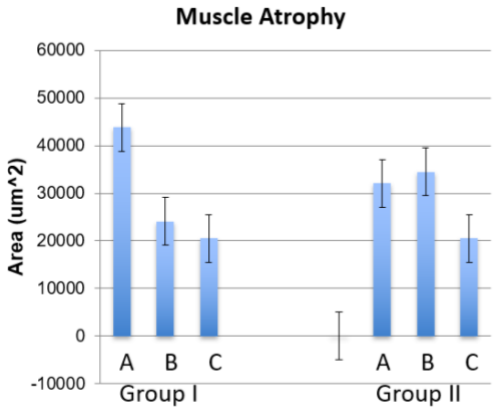

Fig 2: Changes in Muscle Mass and Atrophy. Muscle was cut transversally, fixed, and stained with ant-laminin antibody. In **Fig 2A-C** are images of muscle fibers stained with anti-laminin antibody: **2A**) from an uninjured rat; **2B**) from a rat first injured and then given drug on days 0 and 8; and **2C**) from a rat injured but given no drug. The measuring scale bar represents 50uM. In the bar graph seen in **Fig 2D**, data is derived from analysis of Group 1 (co-apted, left), of Group 2 (nerve sutured to muscle, right) and un-surgerized rats (control, not seen). For Group 1, the difference between drug and no drug (A,B) is p=0.05; for Group 2, drug vs no drug (A,B) is p=0.799. Drug treatment in rats with transected nerves but sutured to the muscle wall showed no effect on muscle mass. On the other hand, co-apted nerves post-transection did show a drug effect leading to an increase in muscle size which was over a 2-fold increase in muscle mass.

3. Scarring Around Nerve Fibers

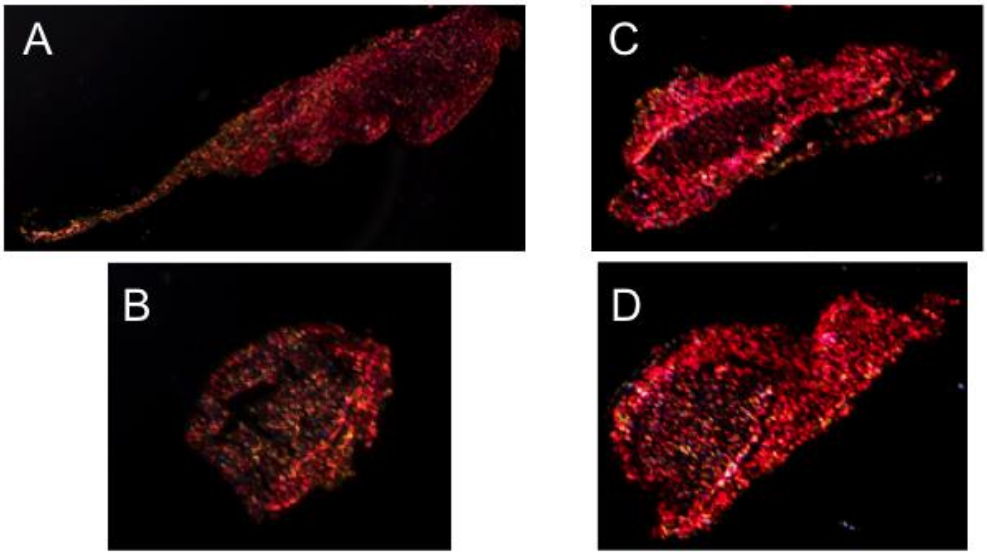

Figure 3. Proximal nerve sections were stained with Picro Sirius Red (PSR). An injured proximal nerve from two mice treated with drug can be seen in **Fig 3A** and **3B**; an example of injured proximal nerve from to mice without drug can be seen in **Fig 3C** and **3D**. **Figs 3A,B** showed a higher level of green fibers indicating Collagen type I. **Figs 3C,D** showed more red/yellow areas indicating Collagen type III associated with scar formation. Images were analyzed using ImageJ.

4. Grip Strength Recovery

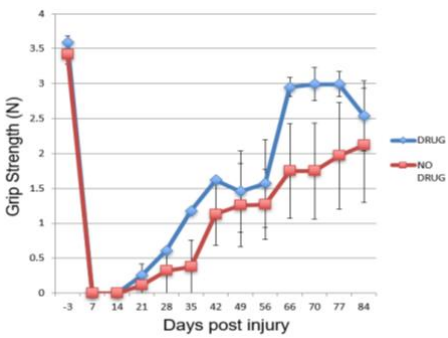

Fig 4A

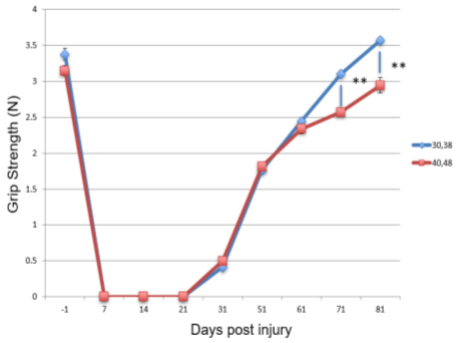

Fig 4B

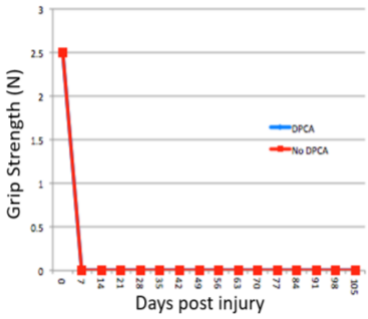

Fig 4C

Figure 4: Recovery of Grip Strength. As seen in **Fig 4A**, without drug, grip strength (N) showed recovery over 84 days though not complete (2.1 vs 3.5). With drug given on day 0 & 8, a drug effect is seen on day 56, but by day 66, the response plateaus and then drops. We decided to re-inject drug to avoid this plateau effect. In **Fig 4B**, we gave a second round of drug on days 30&38 or days 40&48. Not only did we eliminate the plateau effect, but we saw a total recovery of grip strength. By day 81, day 30&38 re-injection had surpassed drug at day 40&48 re-injection and had surpassed the original grip strength and was statistically significant. In **Fig 4C**, we compared drug vs no drug in groups with nerve sutured to muscle (our negative control). In all cases, no return of grip strength was seen.

We had asked for a one year no cost extension. Though we were able to generate more data, we still have more data that needs to analyzed before a paper will be submitted.

5. Drug Delivery Technology Development (Aims 3 and 4)

We optimized a PEG-DPCA prodrug system and developed new formulations for localized delivery of DPCA. The PEG-DPCA prodrugs used in the in-vivo digit studies described above include a biocompatible polymer coupled to DPCA via a trivalent ester linker for hydrolysis and release of DPCA in-vivo (**Figure 5A**). Dissolving **P7D3** and **P80D6** in water results in an injectable gel with high drug loading.

During the grant period we optimized the synthesis strategy as part of a structure-property relationship study. The optimized synthesis involves conversion of hydroxyl terminated PEG to carboxylic acid terminated PEG using TEMPO, insertion of the trivalent Tris linker, followed by coupling of CDI-activated DPCA. Detailed characterization of **P7D3** by mass spectrometry revealed sub-quantitative conjugation of 1,4-DPCA to the PEG (i.e. slightly <3 1,4-DPCA per PEG). Reaction temperature, reagent concentrations and reaction times were shown to have a significant impact on coupling efficiency, allowing us to minimize batch-to-batch variability.

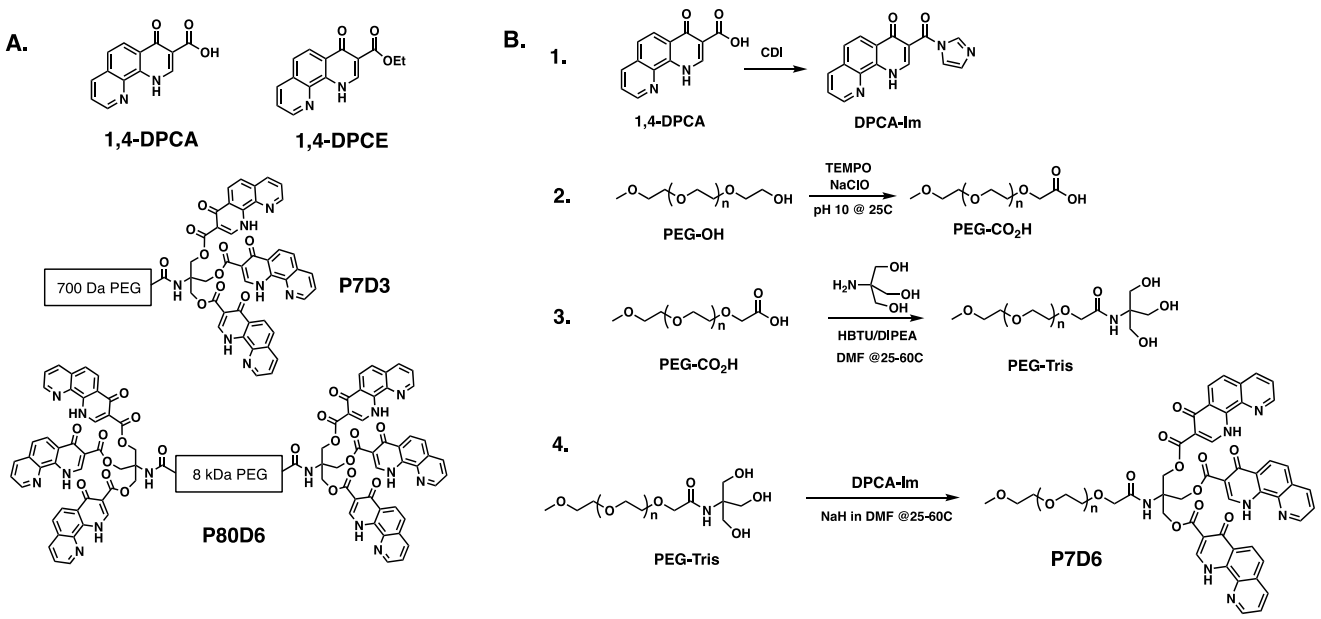

Figure 5. Scheme showing (A) the chemical structures of 1,4-DPCA, 1,4-DPCE and PEG-DPCA prodrugs **P7D3** and **P80D6**; and (B) the optimized synthetic approach.

Both **P7D3** and **P80D6** were synthesized using this approach in multigram quantities, mixed together in a mole ratio 53:47 (P7D3:P80D6) and hydrated to produce a gel with shear-thinning behavior. Structural investigations revealed the presence of nanofibers as a consequence of PEG-DPCA self-assembly to form DPCA-rich nanofiber cores due to the hydrophobicity of 1,4-DPCA. This nanogel formulation was used in the digit regeneration studies described above.

Another goal was to develop alternatives delivery systems for DPCA that would include bioadhesive components for localization within a target tissue. One of the new formulations developed was poly(lactic-co-glycolic acid) (PLGA) polymer microparticles for sustained release of 1,4-DPCA. We originally proposed to use an oil-in-water emulsion technique in which a solution of PLGA and DPCA is dispersed in water followed by evaporation of the organic solvent to yield drug-entrapped PLGA microparticles. An unexpected discovery was that PLGA and 1,4-DPCA were not mutually soluble in any organic solvents, rendering this approach impossible. To solve this problem, we synthesized the ethyl ester derivative of 1,4-DPCA, 1,4-DPCE (**Figure 5A**), which hydrolyzes in the presence of water to yield the active drug 1,4-DPCA.

DPCE loaded PLGA particles were created by a single emulsion technique. 5-10kDa PLGA polymer was dissolved in dichloromethane (DCM) at a concentration of 1.25% (w/v), and DPCE was added to the organic phase at a concentration of 0.1% (w/v). Polyvinyl alcohol was dissolved in Milli-Q water to yield a 0.2% (w/v) solution which will be referred as the aqueous phase. The organic solution was added dropwise to the aqueous phase in which the final volume ratio was 0.5 of organic phase to aqueous phase. This suspension was homogenized by ultrasonication and left to stir overnight for evaporation of the organic solvent. The resulting suspension was centrifuged at 5000 rpm three times for 30 minutes with water washes in between each centrifugation step. The resulting particles were characterized by SEM (**Figure 6**), revealing an average particle size of 273 +/- 10 nm.

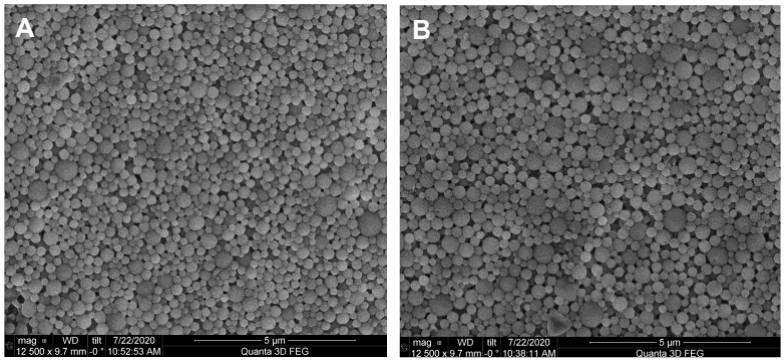

Figure 6. SEM characterization of PLGA (A) and DPCE-entrapped PLGA (B) microparticles.

Release of DPCE from PLGA microparticles was characterized by placing microparticles inside a 3500 MWCO dialysis membrane. The dialysis membrane and outer compartment were filled with Milli-Q water at a final volume ratio of 0.0375. At specific time intervals, small volumes of the outer compartment were collected and the amount of DPCE present was measured by HPLC analysis. As can be seen in **Figure 7**, DPCE was gradually released over approximately 24 hours using this method. In the future we plan to optimize the microparticle formulation to achieve more extended release of entrapped drug.

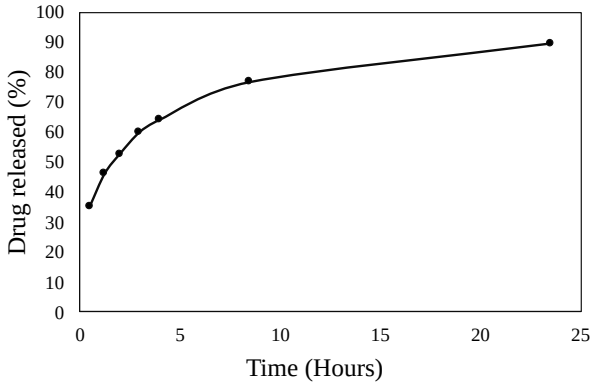

Figure 7. In-vitro release of 1,4-DPCE from PLGA microparticles.

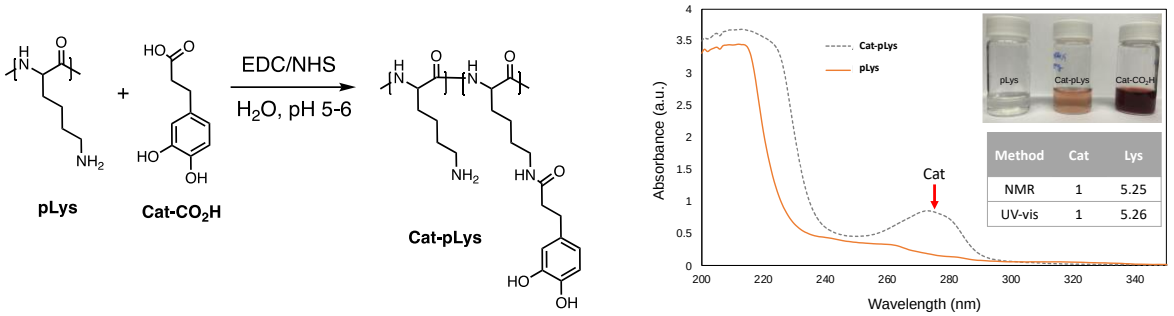

Figure 8. Synthesis and characterization of DOPA-pLys. Shown on the left is the synthetic approach involving conjugation of a catecholic acid to pLys using EDC/NHS chemistry. Shown on the right are characterizations of Cat-pLys. Analysis by UV-vis shows emergence of a 280nm peak indicative of catechol. The inset photo shows the orange color characteristic of catechols treated with Arnow stain. NMR and UV-vis analyses reveal about 1 Cat for every 5 Lys residues.

***Bioadhesive Coatings for 1,4-DPCA Delivery*.**

A desired feature of these microparticles for oral or local delivery of 1,4-DPCA or 1,4-DPCE is tissue adhesion. Microparticles for delivery into a wound site should be tissue adhesive in order to prevent microparticle migration and to localize drug release to the intended location. To enhance bioadhesion, we prepared PLGA microparticles with a bioadhesive coating inspired by mussel adhesive proteins. For attachment to wet surfaces, mussels secrete specialized protein glues that are rich in lysine (Lys) and the unusual amino acid 3,4-dihydroxyphenylalanine (DOPA). The adhesive component of DOPA is the 3,4-dihydroxyphenyl side chain, known as catechol (Cat). Native mussel adhesive proteins and synthetic polymers containing DOPA/Cat and Lys have been shown to be highly adhesive to tissue surfaces. We therefore synthesized a Cat-modified lysine polymer mimic of mussel adhesive protein (Cat-pLys) to be applied to 1,4-DPCA/1,4-DPCE microparticles as a bioadhesive coating (**Figure 8**). Cat-pLys was characterized by NMR, UV-vis and Arnow stain (a catechol-sensitive colorimetric dye) confirming the presence of catechol at a ratio of 1:5.25 (Cat:Lys).

To evaluate bioadhesion, PLGA microparticles were created by a single emulsion technique and Cat-pLys coated on the surface by adsorption from solution. Mucoadhesion was evaluated by a high throughput technique in which a microparticle suspension was added to a microplate well containing adsorbed mucin as a simple mimic of a mucosal tissue surface. After exposure for several hours, the plate was inverted and spun in a centrifuge to remove unattached particles by centrifugal force. Subsequently the remaining attached particles could be quantified by image analysis using ImageJ. The

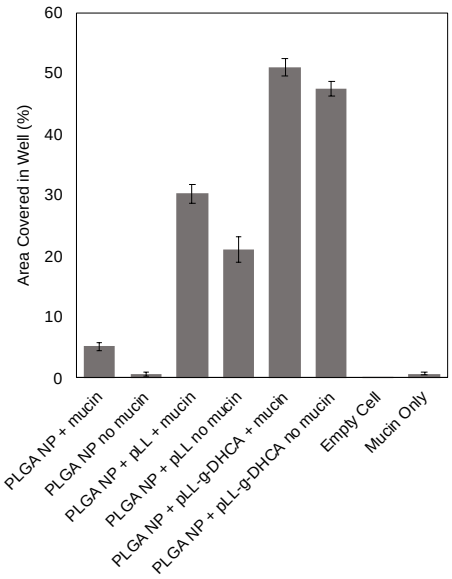

Figure 9. A mucoadhesion assay showed that a Cat-pLys coating dramatically improved PLGA microparticle mucoadhesion compared to uncoated or pLys coated microparticles.

results (**Figure 9**) showed that unmodified PLGA microparticles were not adhesive to the mucin surface whereas pLys coated particles showed enhanced adhesion. However, the highest adhesion was observed for Cat-pLys coated microparticles, demonstrating the adhesive nature of Cat-pLys coated PLGA microparticles.

A second approach to improving bioadhesion and altering release kinetics of 1,4-DPCA/1,4-DPCE is to directly coat drug crystals with a bioadhesive coating for use as a topical or oral delivery system. For this purpose we utilized a mussel-inspired catecholamine coating called polydopamine (PDA), which deposits spontaneously from aqueous solution as a conformal coating on surfaces (Messersmith et al., Science, 2007). We crystallized 1,4-DPCE crystals and deposited a thin coating of PDA by immersion for up to 24 hours in an alkaline aqueous solution of dopamine.HCl. 1,4-DPCE crystals were found to be coated with a thin PDA film, thus providing a potential tissue adhesive surface to the crystals (**Figure 10**). Interestingly, we discovered that the PDA coating provided a tool for altering drug release from the crystals of 1,4-DPCE (**Figure 11**).

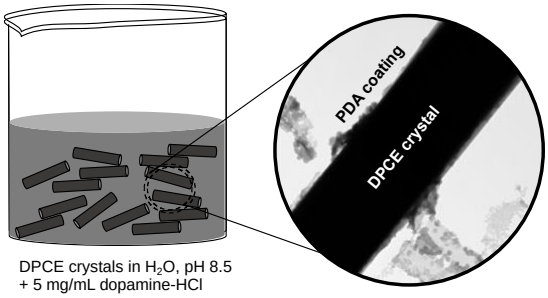

Figure 10. A mucoadhesion assay showed that a Cat-pLys coating dramatically improved PLGA microparticle mucoadhesion compared to uncoated or pLys coated microparticles.

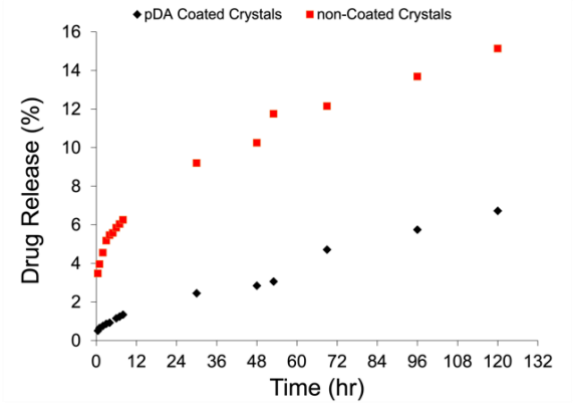

Figure 11. In-vitro drug release studies showed that a PDA coating altered the kinetics of drug release from 1,4-DPCE crystals.

Another method for making bioadhesive nanoparticles for delivery of 1,4-DPCA involves the synthesis of block copolymers that self-assemble into nanoparticles with a hydrophobic core

Figure 12. Block copolymers for self-assembly into mucoadhesive nanoparticles. The blue structures are catechol and amine mimics of mussel adhesive proteins and are water soluble, whereas the red portion is hydrophobic. In water, the polymer forms nanoparticles with a hydrophobic core (red) and a bioadhesive surface (blue). These nanoparticles are stable in suspension as shown in the middle photograph, and are composed of ~220nm particles as shown in the electron micrograph at right.

and a surface of catechol and amine for bioadhesion (**Figure 12**). We expect that the hydrophobic core can be loaded with drug for topical or oral delivery of 1,4-DPCA.

Finally, we also synthesized peptide and ester conjugates of 1,4-DPCA with L-3,4-dihydroxydopamine (DOPA) and related compounds that contain catechol, the peptide constituent of mussel adhesive proteins that is known to be adhesive to tissue surfaces. Due to the reactivity of the catechol, protecting group chemistries were employed in multi-step reactions, followed by terminal cleavage of protecting group to yield the catechol conjugates. One construct was designed with a glycerol core conjugated to two DOPA residues and one DPCA (**Figure 13**). High impurity and low yield prevented us from achieving a pure product and we abandoned this approach. A second approach was more successful, involving direct conjugation of dihydrocaffeic acid to DPCA (**Figure 14**). The DPCA-catechol product was isolated in high purity, but unfortunately this construct proved intractable due to insolubility in water and most organic solvents.

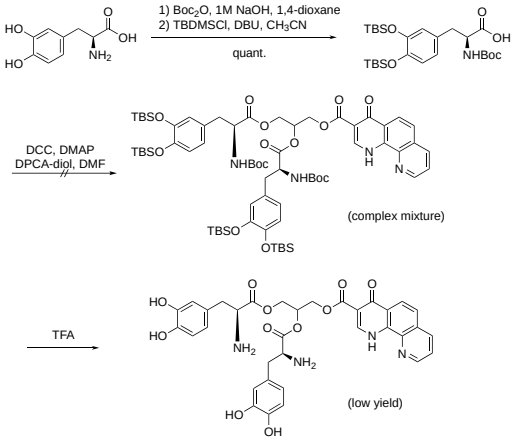

Figure 13. Synthesis of DOPA peptide conjugate of DPCA. High impurity and low yield

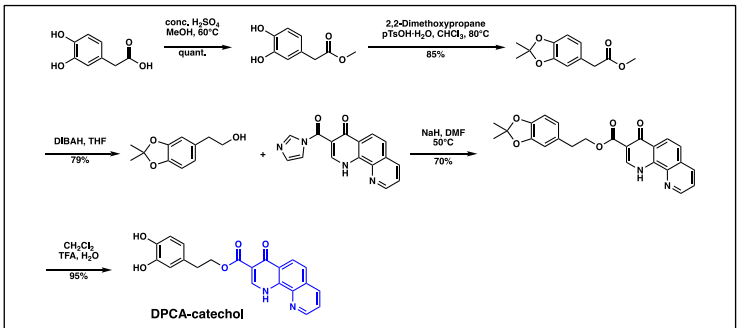

Figure 14. Synthesis of DPCA-catechol, a bioadhesive conjugate of DPCA.

Conclusion

The ability of 1,4-DPCA-PEG to accelerate and prolong nerve growth is quite evident. During the timepoints examined, drug activity was clear in terms of myelinated nerve regeneration, inhibition of Wallerian degeneration and restoration of functional activity as measured by grip strength. Furthermore, the drug counters muscle atrophy and leads to increased muscle fiber growth and blocks scar formation.

For all of these nerve resection studies, the Giladi laboratory has been consulting with Dr. Tuffaha of the Brandacher laboratory (3,4) who has guided us through the histological and functional analysis.

We believe that these studies are ready for large animal studies and then an IND for a clinical trial.

What opportunities for training and professional development has the project provided?

In the Messersmith laboratory. Kelsey DeFrates carried out the studies related to this project as a graduate student, obtained her PhD and is now doing postdoctoral studies at UCSF.
In the Giladi laboratory, Bosung Titanji, MS, did much of the surgery and preparation of tissue samples. She is now in medical school at Meharry in Nashville.
In the Heber-Katz Laboratory, Sam Bollinger, BS in Chemistry from Penn State went to Stanford for a PHD after LIMR. Elan Zebrowitz was came to the lab with BS from Muhlenberg College and went to NY Medical College for an MD after LIMR. Ben Cameron, who came to the lab with a MS in T cell Immunology, went to Univ of Pittsburgh Graduate School in Cancer Biology after leaving LIMR. All participated to some degree in this project.

How were the results disseminated to communities of interest?

A manuscript is in the process of being written up.

IMPACT

We expect that once the studies are complete and the results published, there will be a significant impact.

CHANGES/PROBLEMS N/A

PRODUCTS

Publications, conference papers, presentations

Publications:

Bedelbaeva K, Cameron B, Latella J, Aslanukov A, Gourevitch D, Davuluri R, and Heber-Katz E. 2023. Epithelial-Mesenchymal Transition: An Organizing Principle of Mammalian Regeneration. Frontiers in Cell and Developmental Biology. 11: doi.org/10.3389 /fcell.2023.1101480.

K. DeFrates, J. Engstrom, N.A. Sarma, A. Umar, J. Shin, W. Xie, D. Pochan, A. Omar, P.B. Messersmith, “The influence of molecular design on structure-property relationships of a supramolecular polymer prodrug”, Proceedings of the National Academy of Sciences USA, e2208593119 (2022). doi.org/10.1073/pnas.2208593119

DeFrates KG, Tong E, Cheng G, Heber-Katz E, Messersmith PB. 2023. A pro-regenerative supramolecular prodrug protects against and repairs colon damage in experimental colitis. Advanced Science, in press.

Conference paper:
Bedelbaeva K, Giladi AM, Azlanukov A, Tufaha S, Chen J, Messersmith PB, and Heber-Katz, E. 2023. Effect of DPCA/PEG, a Metabolic Modulator, on Nerve Regeneration post Transection in the Rat Forelimb (MHSRS Abstract #255/Poster).

Presentations:
Heber-Katz E. "Metabolic Reprogramming:Downstream targets" at the World Stem Cell Summit, Wake Forrest, NC. June, 2023.

PARTICIPANTS AND OTHER COLLABORATING ORGANIZATIONS

1. Heber-Katz E, PhD at Lankenau Institute for Medical Research, Wynnewood, PA.
2. Aviram Giladi, MD, MS at the Curtis Hand Center, Medstar Hospital, Baltimore, MD
3. Phillip Messersmith, PhD at UC Berkeley, Berkeley CA

General References

1.Clark LD, Clark RK, Heber-Katz E. 1998. A new murine model for mammalian wound repair and regeneration. Clin Immunol Immunopathol 88: 35-45. PMID: 9683548.
2.Arthur LM, Sachadyn P, Gourevitch D, Heber-Katz E. 2011. Cardinal Regenerative Features of the MRL Mouse – An Update. Gene Therapy and Regulation 6:51-70.
3.Yu L, Han M, Yan M, Lee J, Muneoka K. 2012. BMP2 induces segment-specific skeletal regeneration from digit and limb amputations by establishing a new endochondral ossification center Developmental Biology 372:263-273.
4.Yu L, Dawson LA, Yan M, Zimmel K, Lin Y-L, Dolan CP, Han M, Muneoka K. 2019. BMP9 stimulates joint regeneration at digit amputation wounds in mice, Nature Communications. 41467: 8278-4.
5.Zhang, Bedelbaeva K, Strehin I, Gourevitch D, Messersmith PB, Heber-Katz E. 2015. Drug-induced Regeneration in Adult Mice. Science Transl Med. 7:290 PMID:26042709.
6.Cheng J, Amin D, Latona JA, Heber-Katz E, Messersmith PB. 2019. Supramolecular Polymer Hydrogels for Drug-induced Tissue Regeneration. ACS Nano. 13:5493-5501. PMID: 31067407.
7.Nagai K, Ideguchi H, Kajikawa T, Li X, Chavakis T, Cheng J, Messersmith PB, Heber-Katz E and Hajishengallis G. 2020. An injectable hydrogel-formulated inhibitor of prolyl-4-hydroxylase promotes T regulatory cell recruitment and enhances alveolar bone regeneration during resolution of experimental periodontitis. FASEB Journal. 34: 13726-13740.
8.Zebrowitz E., Aslanukov A., Kajikawa T., Bedelbaeva K, Bollinger, S., Zhang, Y, Sarfatti D., Cheng, J., Messersmith, PB, Hajishengallis G., Heber-Katz E. 2022. Prolyl-hydroxylase inhibitor-induced regeneration of alveolar bone and soft tissue in a mouse model of periodontitis through metabolic reprogramming. Frontiers in Dental Medicine-Regenerative Dentistry, doi.org/10.3389/fdmed.2022.992722
9.Latona J, Shah A, Cheng J, Messersmith P, Heber-Katz E. 2017. Enhanced Liver Regeneration After Partial Hepatectomy in Mice Treated with a Prolyl Hydroxylase Inhibitor. *Am J Transplant.*17 (suppl 3).

10.Tuffaha SH …Brandacher G. 2016. Growth Hormone Therapy Accelerates Axonal Regeneration, Promotes Motor Re-innervation, and Reduces Muscle Atrophy following Peripheral Nerve Injury. Plast. Reconstr. Surg. 137: 1771.
11. Kern B, Budihardjo JD, Mermulla S, Quan A, Cadmi C, Lopez J, Khusheim M, Xiang S, Park J, Furtmüller GJ, Sarhane KA, Schneeberger S, Lee WP, Hoke A, Tuffaha SH, Brandacher G. 2017. A Novel Rodent Orthotopic Forelimb Transplantation Model That Allows for Reliable Assessment of Functional Recovery Resulting From Nerve Regeneration. Am J. Transplant 17: 622-634.
12. Bedelbaeva K, Giladi AM, Azlanukov A, Tufaha S, Chen J, Messersmith PB, and Heber-Katz, E. 2023. Effect of DPCA/PEG, a Metabolic Modulator, on Nerve Regeneration post Transection in the Rat Forelimb (Abstract #255/Poster).
13. Bedelbaeva K, Cameron B, Latella J, Aslanukov A, Gourevitch D, , Davuluri R, and Heber-Katz E. 2023. Epithelial-Mesenchymal Transition: An Organizing Principle of Mammalian Regeneration. Frontiers in Cell and Developmental Biology. 11: doi.org/10.3389 /fcell.2023.1101480.
14. DeFrates KG, Tong E, Cheng G, Heber-Katz E, Messersmith PB. 2023. A pro-regenerative supramolecular prodrug protects against and repairs colon damage in experimental colitis. Advanced Science, in press.